

Electronic Supplementary Information

High efficient constant-voltage triboelectric nanogenerator

Xinyuan Li,^{‡^a} Chuguo Zhang,^{‡^{ab}} Yikui Gao,^{‡^{ac}} Zhihao Zhao,^a Yuexiao Hu,^{ac} Ou Yang,^{ab}
Lu Liu,^{ab} Linglin Zhou,^{ab} Jie Wang,^{*^{abc}} and Zhong Lin Wang^{*^{abcd}}

^aCAS Center for Excellence in Nanoscience, Beijing Key Laboratory of Micro-nano Energy and Sensor, Beijing Institute of Nanoenergy and Nanosystems, Chinese Academy of Sciences, Beijing 100083, P. R. China. E-mail: wangjie@binn.cas.cn

^bSchool of Nanoscience and Technology, University of Chinese Academy of Sciences, Beijing 100049, P. R. China.

^cCenter on Nanoenergy Research, School of Physical Science and Technology, Guangxi University, Nanning, 530004, P. R. China

^dSchool of Materials Science and Engineering, Georgia Institute of Technology, Atlanta, GA 30332-0245, USA. E-mail: zhong.wang@mse.gatech.edu

† Electronic Supplementary Information (ESI) available. See DOI: 10.1039/x0xx00000x

‡ These authors contributed equally to this work.

Content

Supplementary Figures:

Fig. S1. Detailed structure of PV-TENG and CV-TENG in top view.

Fig. S2. The circuit connection of CV-TENG and PV-TENG.

Fig. S3. Schematic current and voltage superposition of PV-TENG.

Fig. S4. Electrical performance of PV-TENG and CV-TENG. Voltage changes versus frequencies of (a) PV-TENG and (b) CV-TENG. Current changes versus frequencies of (c) PV-TENG and (d) CV-TENG.

Fig. S5. The detailed current information involving average current, peak current and crest factor of CV-TENG.

Fig. S6. Peak power and average power of CV-TENG changes versus different resistance load.

Fig. S7. Voltage of PV-TENG changes versus different resistance load.

Fig. S8. Voltage of CV-TENG changes versus different resistance load.

Fig. S9. Average current and average power of CV-TENG and PV-TENG at different frequencies. Average current changes versus different resistance load at (a) 0.5 Hz, (b) 1.0 Hz, and (c) 2.0 Hz, respectively. Average power changes versus different resistance load at (d) 0.5 Hz, (e) 1.0 Hz, and (f) 2.0 Hz, respectively.

Fig. S10. Energy ratio between CV-TENG and PV-TENG.

Fig. S11. Average power changes versus voltage at different frequencies charged by (a) PV-TENG and (b) CV-TENG with capacitance load.

Fig. S12. The circuit diagram of TENG charging capacitor.

Fig. S13. The relationship between COMSOL data and motion path state of free-standing mode TENG. (a) COMSOL data of free-standing mode TENG at different motion path state. (b) TENG's voltage changes versus motion path in free-standing mode TENG. (c) The schematic diagram of TENG's voltage changes versus motion path in free-standing mode TENG.

Fig. S14. Circuit connection of (a) PV-TENG and (b) CV-TENG.

Fig. S15. Two methods of power management for TENG.

Fig. S16. The circuit diagram of CV-TENG charging capacitor.

Fig. S17. The relationship between gap distance and electrical output of TENG.

Supplementary Table:

Table S1. The performance of TENG in this work compared with others based on phase shift design.¹⁻⁶

Table S2. Detailed value of peak, trough and average current of PV-TENG changes versus different resistance.

Table S3. Detailed value of peak, trough and average current of CV-TENG changes versus different resistance.

Supplementary Notes:

Note S1. Average power comparison of TENG.

Note S2. Formula derivation of stored energy and electric quantity of the capacitor.

Note S3. Electrical model of TENG.

Note S4. Relationship between the voltage of TENG and motion path.

Note S5. Power management of CV-TENG.

Supplementary Movies:

Movie S1 Comparison between CV-TENG and PV-TENG to power 132 LEDs.

Movie S2 Four white lights are continuously powered by CV-TENG.

Movie S3 Four multifunction digital hygrometers can work continuously by using CV-TENG.

Supplementary Figures

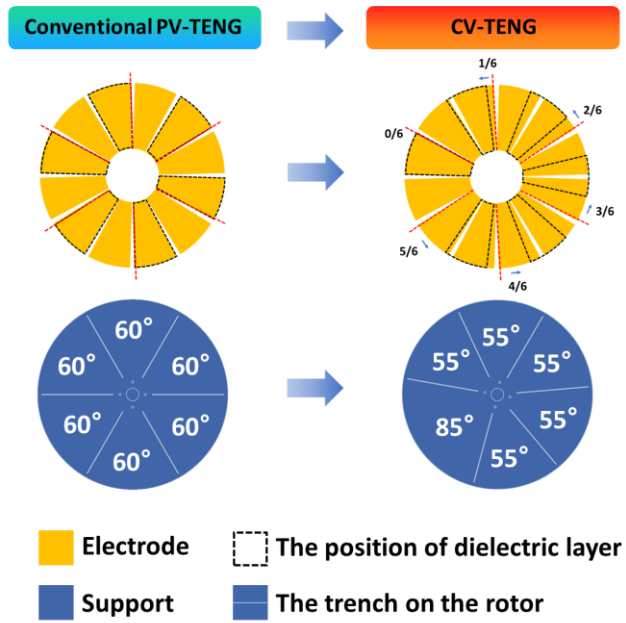


Fig. S1. Detailed structure of PV-TENG and CV-TENG in top view.

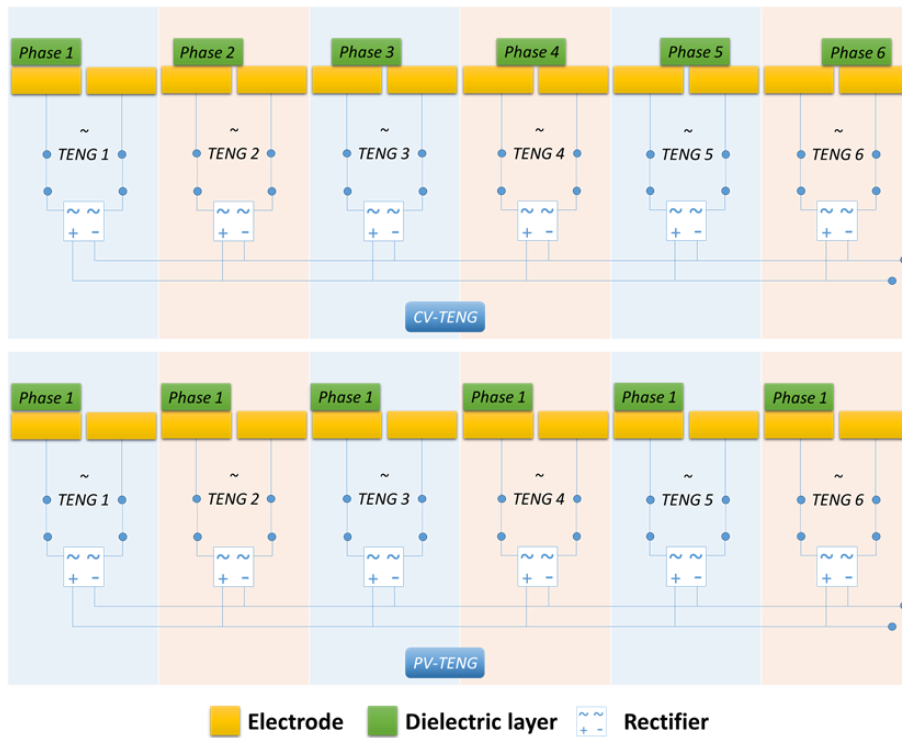


Fig. S2. The circuit connection of CV-TENG and PV-TENG.

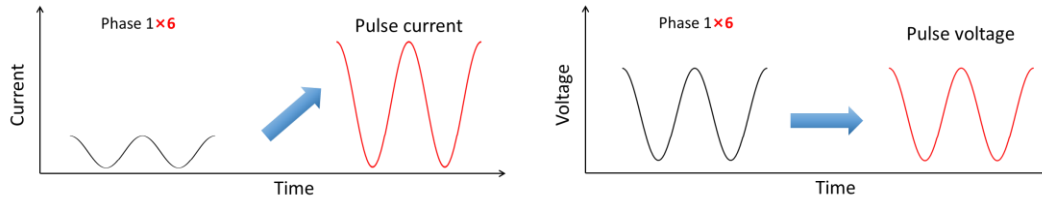


Fig. S3. Schematic current and voltage superposition of PV-TENG.

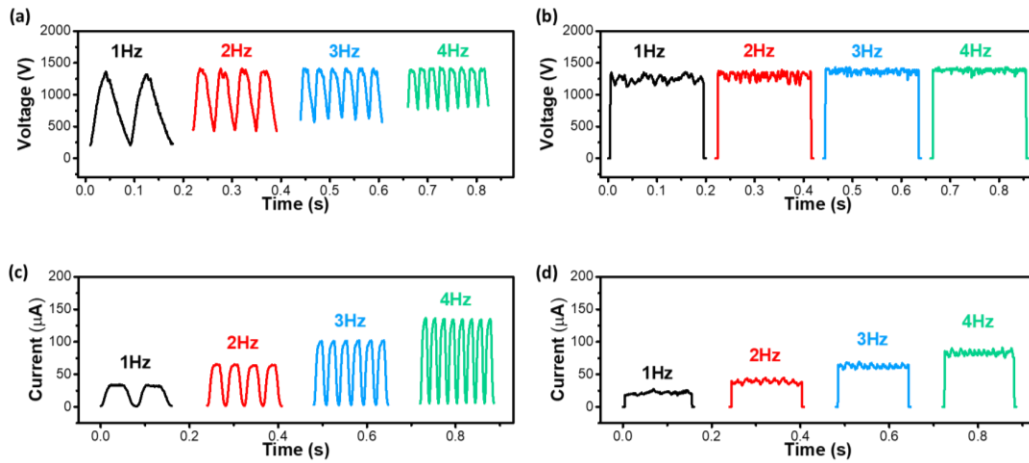


Fig. S4. Electrical performance of PV-TENG and CV-TENG. Voltage changes versus frequencies of (a) PV-TENG and (b) CV-TENG. Current changes versus frequencies of (c) PV-TENG and (d) CV-TENG.

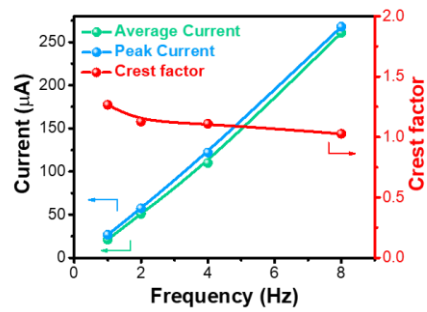


Fig. S5. The detailed current information involving average current, peak current and crest factor of CV-TENG.

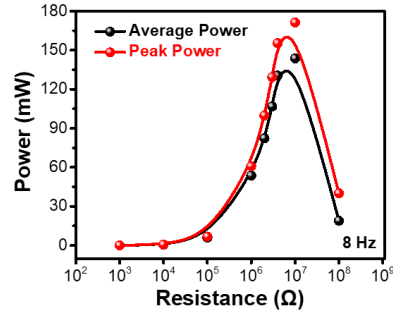


Fig. S6. Peak power and average power of CV-TENG changes versus different resistance load.

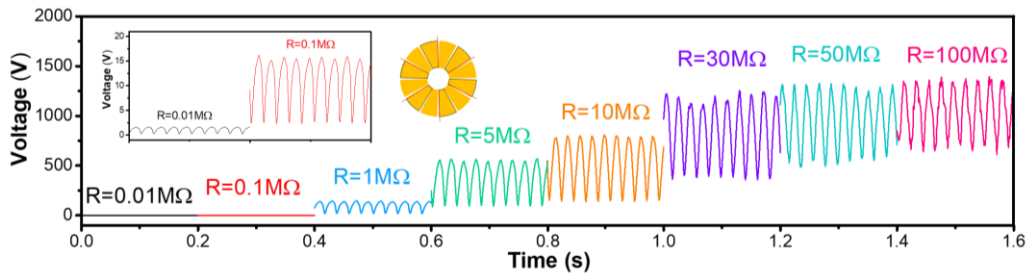


Fig. S7. Voltage of PV-TENG changes versus different resistance load.

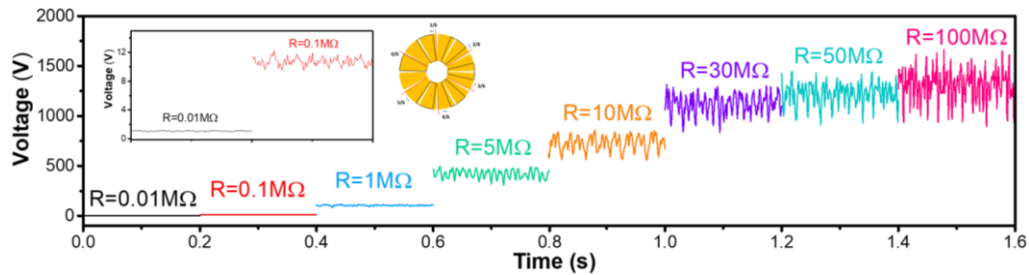


Fig. S8. Voltage of CV-TENG changes versus different resistance load.

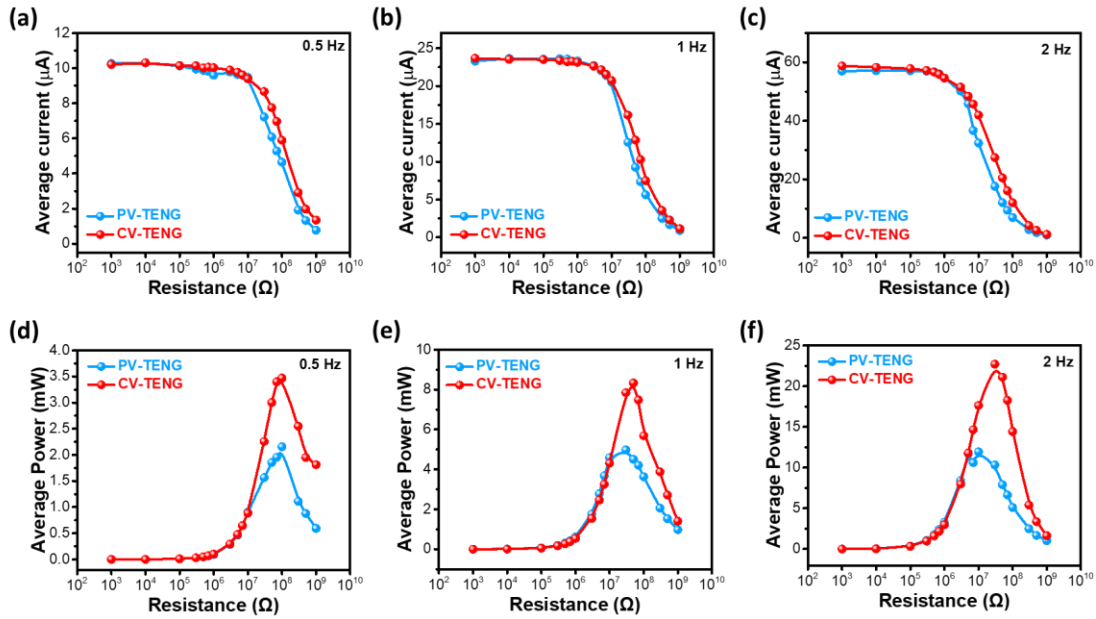


Fig. S9. Average current and average power of CV-TENG and PV-TENG at different frequencies. Average current changes versus different resistance load at (a) 0.5 Hz, (b) 1.0 Hz, and (c) 2.0 Hz, respectively. Average power changes versus different resistance load at (d) 0.5 Hz, (e) 1.0 Hz, and (f) 2.0 Hz, respectively,

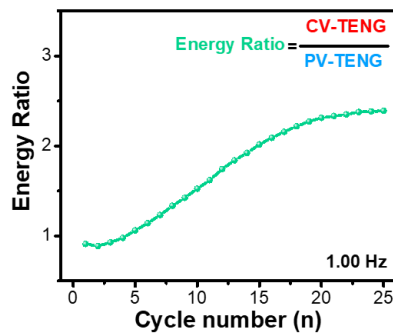


Fig. S10. Energy ratio between CV-TENG and PV-TENG.

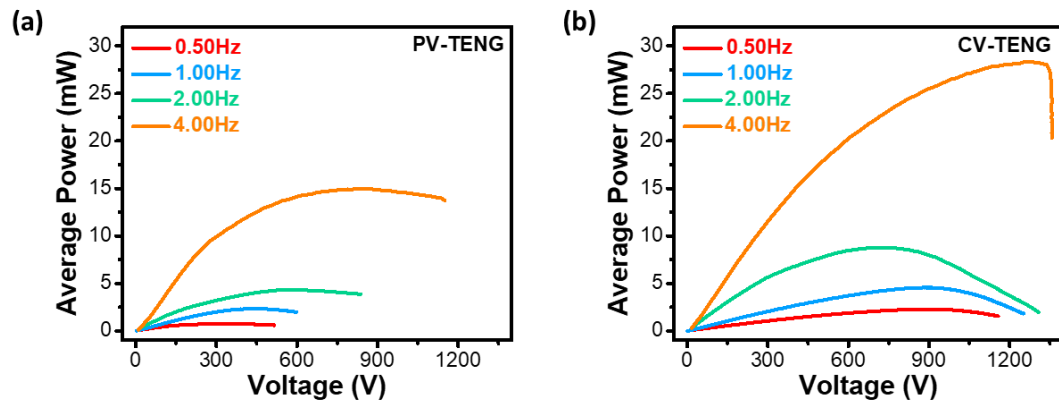


Fig. S11. Average power changes versus voltage at different frequencies charged by (a) PV-TENG and (b) CV-TENG with capacitance load.

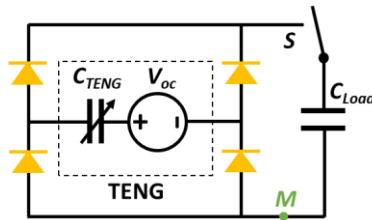


Fig. S12. The circuit diagram of TENG charging capacitor.

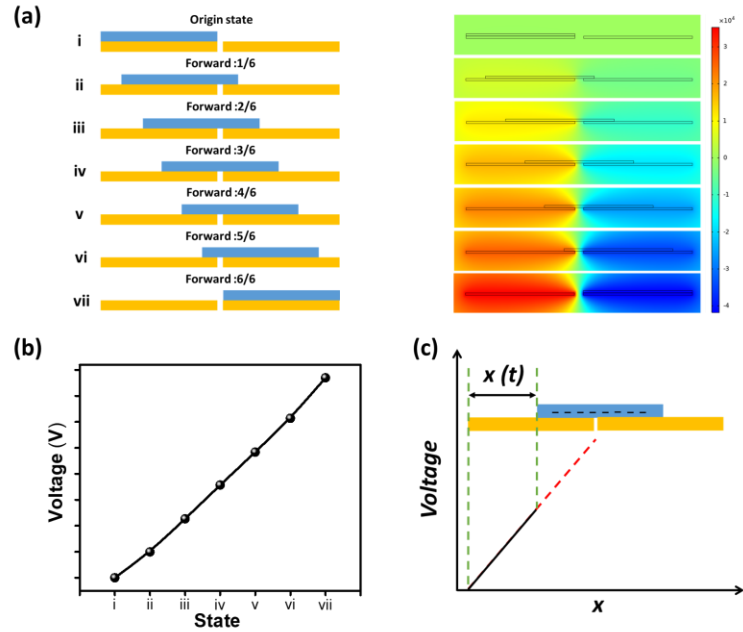


Fig. S13. The relationship between COMSOL data and motion path state of free-standing mode TENG. (a) COMSOL data of free-standing mode TENG at different motion path state. (b) TENG's voltage changes versus motion path in free-standing mode TENG. (c) The schematic diagram of TENG's voltage changes versus motion path in free-standing mode TENG.

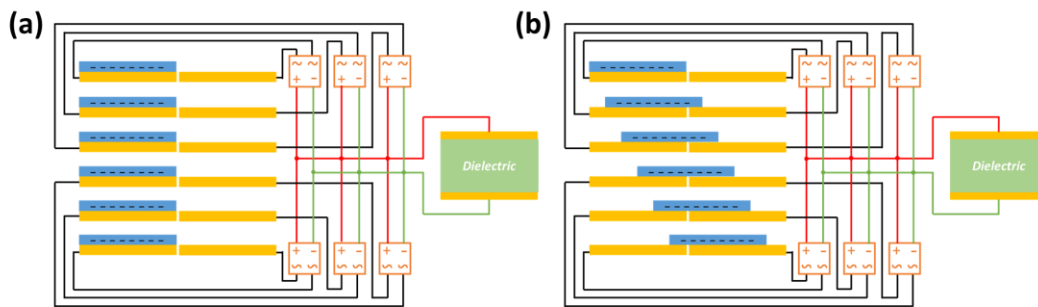


Fig. S14. Circuit connection of (a) PV-TENG and (b) CV-TENG.

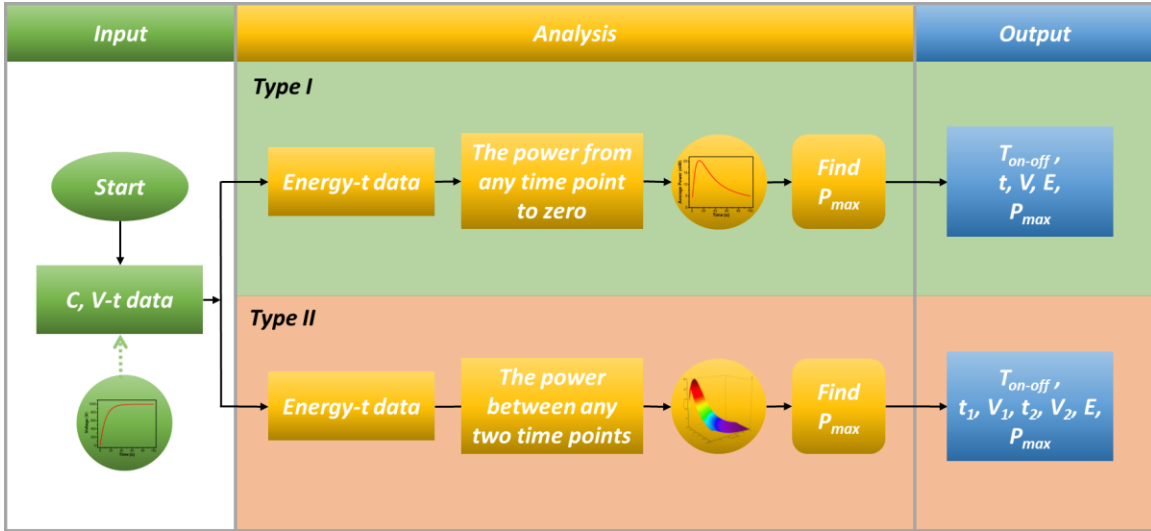


Fig. S15. Two methods of power management for TENG.

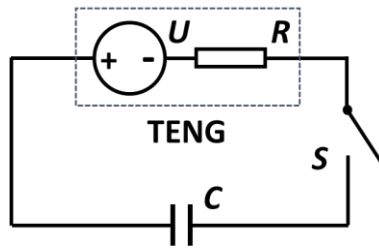


Fig. S16. The circuit diagram of CV-TENG charging capacitor.

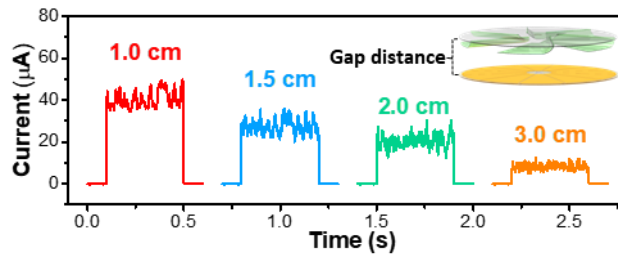


Fig. S17. The relationship between gap distance and electrical output of TENG.

Supplementary Tables

Table S1. The performance of TENG in this work compared with others based on phase shift design.¹⁻⁶


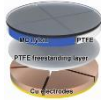


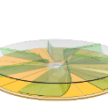
TENG structure	TENG Size	Rotation speed (Hz)	Average power	Crest factor	Reference
	508.7 cm ⁻³	8	4.42 (W·m ⁻³ ·Hz ⁻¹)	1.31	[1]
	78.5 cm ⁻²	15.33	40.6 (mW·m ⁻² ·Hz ⁻¹)	1.26	[2]
	678.2 cm ⁻³	8.33	2.0 (W·m ⁻³ ·Hz ⁻¹)	1.10	[3]
	19.6 cm ⁻²	12.5	98 (mW·m ⁻² ·Hz ⁻¹)	1.09	[4]
	705.9 cm ⁻³	10	0.29 (W·m ⁻³ ·Hz ⁻¹)	1.08	[5]
	113.04 cm ⁻²	5	222 (W·m ⁻² ·Hz ⁻¹)	1.05	[6]
	706.5 cm ⁻² 706.5 cm ⁻³	8	254 (mW·m⁻²·Hz⁻¹) 25.4 (W·m⁻³·Hz⁻¹)	1.03	This work

Table S2. Detailed value of peak, trough and average current of PV-TENG changes versus different resistance.

Resistance (M Ω)	0.01	0.1	1	5	10	30	50	100
Peak current (μ A)	160.25	157.80	139.99	111.11	79.88	40.50	25.97	13.61
Valley current (μ A)	24.72	23.21	18.80	18.63	14.32	13.10	1.3	1.47
Average current (μ A)	113.37	111.61	98.17	75.62	53.10	27.92	18.95	10.50

Table S3. Detailed value of peak, trough and average current of CV-TENG changes versus different resistance.

Resistance (M Ω)	0.01	0.1	1	5	10	30	50	100
Peak current (μ A)	117.78	115.32	114.40	93.94	81.80	42.58	26.60	14.91
Valley current (μ A)	96.87	98.28	94.40	72.06	59.56	30.18	21.60	9.65
Average current (μ A)	108.40	107.66	106.22	84.24	72.67	37.26	24.35	13.05

Supplementary Notes

Note S1. Average power comparison of TENGs.

Triboelectric nanogenerator (TENG) plays an increasingly significant role in distributed power sources or self-powered sensors with its remarkable superiority of low cost, easy fabrication, diverse choice of materials, and high efficiency at low operation frequency. Despite average power density is a key character to compare different TENGs fairly, rare research focuses on the standard for TENG as distributed power source. Considering disordered mechanical energy input and a variety of different design styles of TENG, a general-purpose standard of average power is expected to evaluate TENGs as distributed power sources. Here, volume specific average power density per Hertz ($\text{W m}^{-3} \text{Hz}^{-1}$) is proposed as a standard for comparison of average power of different TENGs as distributed power sources. Several works based on phase shift design are compared with the same standard as shown in Fig. 1h, 1i and Supplementary Table 1. It is easy to acquire the device parameter in the style of cylindrical structure TENG, while, it is hard to obtain the height information of planar device because researches pay more attention on charge density every square meter. Therefore, area specific average power density per Hertz ($\text{W m}^{-2} \text{Hz}^{-1}$) is also proposed as a standard for fair comparison in this paper. Meanwhile, previous research has reported the mass specific average power (W kg^{-1}),¹ it is also another suitable standard for fair comparison in terms of considering the mass in practical application of TENG. Therefore, mass specific average power density per Hertz ($\text{W kg}^{-1} \text{Hz}^{-1}$) also could be considered as a standard for comparison of average power of different TENGs as distributed power sources in the future.

Note S2. Formula derivation of stored energy and electric quantity of the capacitor.

The total energy stored in the capacitor (E^C) and the total charge stored in the capacitor (Q^C) can be given by:

$$E^C = \int_0^t P dt = \int_0^t C U_C \frac{dU_C}{dt} dt = \int_0^t C U_C dU_C = \frac{1}{2} C U_C^2 \quad (1)$$

$$Q^C = C U_C \quad (2)$$

where P is the instantaneous power of capacitor, C is the capacitance of the capacitor, U_C represents the voltage of the capacitor. Due to the voltage of the capacitor is a time-varying variable, E^C and Q^C are going to change over time. Energy flowing to the capacitor per cycle and charge flowing to the capacitor per cycle can be derived below:

$$E_n^C = \frac{1}{2}CU_C(n)^2 - \frac{1}{2}CU_C(n-1)^2 \quad (3)$$

$$Q_n^C = CU_C(n) - CU_C(n-1) \quad (4)$$

where n is the cycle number, $V(n)$ is the final voltage value of n cycle.

Note S3. Electrical model of TENG.

As the model established by Niu et al,⁷ Define C_T is the variable capacitor and C_L is capacitance load of TENG, where C_{min} and C_{max} are the minimum and maximum value of variable capacitance of TENG, respectively. It is believed that the charge through node M conforms to the law of charge conservation according to Kirchhoff's law as shown in Fig. S13. Before charging starts, the initial charge on C_T and C_L are zero. The charge on node M is also zero. The mathematical expression is $Q_1^M = 0$, and Q_k^M represents the total charge on node M at the beginning of the k th cycle. The charge (Q_T and Q_L) stored in the capacitor (C_T and C_L) at the end of the first half period in the k th cycle is as follow:

$$Q_{k,1end}^T = C_L \frac{Q_{SC,max} + Q_k^M}{C_L + C_{min}} \quad (5)$$

$$Q_{k,1end}^L = \frac{C_L Q_{SC,max} - C_{min} Q_k^M}{C_L + C_{min}} \quad (6)$$

where $Q_{k,1end}^T$ represents the value at the end of the first half period in the k th cycle. From half period of the first cycle to the beginning of half period of the second cycle, due to the full wave rectifier circuit, the polarity of C_L will be reversed. At the beginning of the second half period of the k th cycle, the charge stored in node M ($Q_{k,mid}^M$) can be given by the following equation:

$$Q_{k,mid}^M = -Q_{k,2begin} + Q_{k,2begin}^C = -Q_{k,1end} - Q_{k,1end}^C \quad (7)$$

The second half cycle is also a one-way charging process. At the end of the second half cycle, the charges stored on C_T and C_L (Q_T and Q_L) can be given by the following equation:

$$Q_{k,2end} = -\frac{C_{max}Q_{k,mid}^M}{C_L+C_{max}} \quad (8)$$

$$Q_{k,2end}^C = -\frac{C_L Q_{k,mid}^M}{C_L+C_{max}} \quad (9)$$

At the end of the second half cycle, the relative polarity of C_L with respect to the TENG is reversed again. Therefore, the charge (Q_{k+1}^M) on the node M at the time of the $k+1$ cycle is given by the following equation:

$$Q_{k+1}^M = -Q_{k+1,1begin} + Q_{k+1,1begin}^C = -Q_{k,2end} - Q_{k,2end}^C \quad (10)$$

By this formula up here, the recursion of Q_k^M can be expressed as

$$Q_{k+1}^M = \frac{C_L-C_{max}}{C_L+C_{max}} \frac{C_L-C_{min}}{C_L+C_{min}} Q_k^M + 2 \frac{C_L-C_{max}}{C_L+C_{max}} \frac{C_L}{C_L+C_{min}} Q_{SC,max} \quad (11)$$

With the boundary condition of $Q_1^M = 0$, the above recursion can be solved as follows:

$$Q_k^M = \frac{C_L-C_{max}}{C_{min}+C_{max}} Q_{SC,max} - \frac{C_L-C_{max}}{C_{min}+C_{max}} Q_{SC,max} \left[\frac{(C_L-C_{max})(C_L-C_{min})}{(C_L+C_{max})(C_L+C_{min})} \right]^{k-1} \quad (12)$$

Therefore, after the first k charging cycle, the voltage $|V_{k,2end}^C|$ on the C_L can be expressed as

$$|V_{k,2end}^C| = \frac{Q_{SC,max}}{C_{min}+C_{max}} \left\{ 1 - \left[1 - \frac{2(C_{min}+C_{max})C_L}{(C_L+C_{max})(C_L+C_{min})} \right]^k \right\} \quad (13)$$

In practical applications, C_L is generally much larger than C_{min} and C_{max} . Using this condition, it can be further simplified as

$$\begin{aligned} |V_{k,2end}^C| &= \frac{Q_{SC,max}}{C_{min}+C_{max}} \left\{ 1 - \exp \left[-\frac{2(C_{min}+C_{max})k}{C_L} \right] \right\} \\ &= \frac{Q_{SC,max}}{C_{min}+C_{max}} \left\{ 1 - \exp \left[-\frac{2(C_{min}+C_{max})ft}{C_L} \right] \right\} \end{aligned} \quad (14)$$

It can be seen from the above formula that the case can be equal to a voltage source with internal resistance charging the same capacitor, and they all follow the same exponential saturation trend. The voltage value can be described as follows:

$$V_{sat} = \lim_{k \rightarrow \infty} |V_{k,2end}^C| = \frac{Q_{SC,max}}{C_{min} + C_{max}} \quad (15)$$

Like the first-order RC charging circuit, independent of C_L , V_{sat} is only a function of the parameters of the TENG.

In the real-time charging behavior of TENG, it is necessary to consider whether the voltage of TENG is higher than the voltage of capacitor when the transferred charge of TENG flowing to the capacitor. Due to constant voltage characteristics of CV-TENG, it is a simplified process to constructing electrical models for CV-TENG charging capacitor for only transferred charge needing to be considered during the charging process.

Note S4. Relationship between the voltage of TENG and motion path.

A model of free-standing mode TENG is fabricated by COMSOL software (Fig. S12a), where TENG consists of two electrode and a dielectric layer. The dielectric layer sliding on the top of electrode to change the electric field distribution between dielectric layer and electrodes. The voltage difference between the two electrodes at each state is collected for further analysis, there is a strong correlation between voltage of open-circuit TENG and motion path as shown in Fig. S12b, which is consistent with previous report.⁸ Therefore, a simple model to describe the relationship between the voltage of TENG and motion path is fabricated as shown in Fig. S12c for further discussion.

Note S5. Power management of CV-TENG.

From the formula (14), CV-TENG can be regard as a constant voltage source with internal resistance as discussed in Note S3. Therefore, electrical model of CV-TENG could be equivalent as the first-order RC charging circuit as shown in Fig. S17. Define the voltage of CV-TENG is U , the inherent resistance of CV-TENG is R , the capacitor is C , the voltage of inherent resistance is U_R , and the voltage of capacitor is U_C . When the switch S is not closed, there is no voltage at both ends of the capacitor, that is, U_C is equal to 0, and the

current (i) in the circuit is 0. In the transient process from the moment the switch S is closed to the capacitor voltage is U_C , the following equation can be listed for the circuit according to Kirchhoff's law:

$$U = U_R + U_C = iR + U_C \quad (16)$$

The charge stored in capacitor is given by the following equation:

$$Q = CU_C \quad (17)$$

Substitute Equation (17) into the current definition of capacitor as follows:

$$i = \frac{dq}{dt} = \frac{d(CU_C)}{dt} = C \frac{dU_C}{dt} \quad (18)$$

Equation (18) is obtained when the reference directions of U_C and i are consistent. It shows that the capacitor current is proportional to the change rate of the capacitor applied voltage.

Substitute Equation (18) into Equation (16) as follows:

$$RC \frac{dU_C}{dt} + U_C = U \quad (19)$$

Equation (19) is a first-order linear differential equation with constant coefficients, it could be solved to obtain the variation rule of capacitor voltage as follows:

$$U_C = U \left(1 - e^{-\frac{t}{RC}} \right) \quad (20)$$

The changing law of circuit current is as follows:

$$i = \frac{U}{R} e^{-\frac{t}{RC}} \quad (21)$$

The voltage of the resistance changes as follows:

$$u_R = iR = \frac{U}{R} e^{-\frac{t}{RC}} \times R = U e^{-\frac{t}{RC}} \quad (22)$$

From the above formula, during the charging process, the voltage of capacitor increases exponentially with time. After a period of time, the capacitor voltage is equal to the

electromotive force of the CV-TENG. While the current of circuit and the voltage of resistance decrease exponentially with time to zero.

The instantaneous power P_C and energy E_C of the capacitor is as follows:

$$P_C = U_C i = C U_C \frac{dU_C}{dt} \quad (23)$$

$$E_C = \int_0^t P dt = \int_0^t C U_C \frac{dU_C}{dt} dt = \int_0^t C U_C dU_C = 0.5 C U_C^2 \quad (24)$$

The charge stored in the capacitor is moved by the electromotive force of the power supply, so the electrical energy E from the power supply is as follow:

$$E = Uq = U C U_C \quad (25)$$

Therefore, the charging efficiency up to time t is as follows:

$$\eta = \frac{E_C}{E} = \frac{0.5 C U_C^2}{U C U_C} = 0.5(1 - e^{-t/RC}) \quad (26)$$

The energy-output efficiency presents very low at the initial stage of charging because the voltage of capacitor is low and the energy output does not increase much. Even the energy-output efficiency is gradually elevated as the time goes by, the maximum energy-output efficiency is only 50%, which is consistent with previous report from V-Q plot.⁹

However, if the capacitor starts charging from the non-zero state, the efficiency will be improved. Here we set the voltage of non-zero is U_0 , increment method is introduced to analyze this phenomenon. The energy increment and charge increment of capacitor are respectively as follows:

$$\Delta E_C = 0.5C[U + (U_0 - U)e^{-t/RC}]^2 - 0.5CU_0^2 \quad (27)$$

$$\Delta q = q(t) - q(0) = C[U + (U_0 - U)e^{-t/RC}] - CU_0 \quad (28)$$

The incremental electric energy from the power source is as follows:

$$\Delta E = U \times \Delta q = UC(U - U_0)(1 - e^{-t/RC}) \quad (29)$$

Therefore, the charging efficiency is as follows:

$$\eta = \frac{\Delta E_C}{\Delta E} = \frac{0.5(U+U_0) - Ue^{-t/RC} + 0.5(U-U_0)e^{-2t/RC}}{U(1-e^{-t/RC})} \quad (30)$$

It is clear that the energy-output efficiency varies with time t and is related to U and U_0 . The energy-output efficiency can be further simplification when the charging behavior ends as follows:

$$\eta = \lim \frac{\Delta E_C}{\Delta E} = \frac{0.5(U+U_0)}{U} \quad (31)$$

Obviously, the above energy-output efficiency is greater than 50% with the voltage U_0 increases. Power management of type II greatly promotes the energy output and even acquires the efficiency close to 100% when U_0 close to U , which breaks through the maximum energy-output efficiency of PV-TENG only up to 50%.

Movie S1 Comparison between CV-TENG and PV-TENG to power 132 LEDs.

Movie S2 Four white lights are continuously powered by CV-TENG.

Movie S3 Four multifunction digital hygrothermographs can work continuously by using CV-TENG.

Reference

1. X. Li, X. Yin, Z. Zhao, L. Zhou, D. Liu, C. Zhang, C. Zhang, W. Zhang, S. Li, J. Wang, and Z. L. Wang, *Adv. Energy Mater.* 2020, **10**, 1903024.
2. H. Ryu, J. Lee, U. Khan, S. Kwak, R. Hinchet, and S. Kim, *Sci.* 2018, **11**, 2057.
3. R. Dharmasena, H. Cronin, R. Dorey, and S. Silva, *Nano Energy* 2020, **75**, 104887.
4. Z. Wu, S. Wang, Z. Cao, R. Ding, and X. Ye, *Nano Energy* 2021, **83**, 105787.
5. J. Wang, Y. Li, Z. Xie, Y. Xu, J. Zhou, T. Cheng, H. Zhao, and Z. L. Wang, *Adv. Energy Mater.* 2020, **10**, 1904227.
6. P. Chen, J. An, R. Cheng, S. Shu, A. Berbille, T. Jiang, and Z. L. Wang, *Energy Environ. Sci.* 2021, **14**, 4523.
7. S. Niu, S. Wang, L. Lin, Y. Liu, Y. Zhou, Y. Hu, and Z. L. Wang, *Energy Environ. Sci.* 2013, **6**, 3576.
8. S. Niu, Y. Liu, X. Chen, S. Wang, Y. Zhou, L. Lin, Y. Xie, and Z. L. Wang, *Nano Energy* 2015, **12**, 760-774.
9. Y. Zi, J. Wang, S. Wang, S. Li, Z. Wen, H. Guo, and Z. L. Wang, *Nat. Commun.* 2016, **7**, 10987.